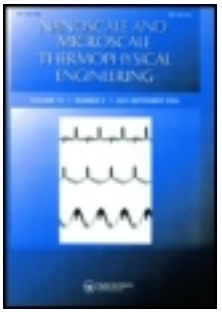

Nanoscale and Microscale Thermophysical Engineering
Publication details, including instructions for authors and subscription information:
http://www.tandfonline.com/loi/umte20

On the Assumption of Detailed Balance in Prediction of Diffusive Transmission Probability During Interfacial Transport

John C. Duda [a], Patrick E. Hopkins [b], Justin L. Smoyer [a], Matthew L. Bauer [a], Timothy S. English [a], Christopher B. Saltonstall [a] & Pamela M. Norris [a]

[a] Department of Mechanical and Aerospace Engineering, University of Virginia, Charlottesville, Virginia

[b] Engineering Sciences Center, Sandia National Laboratories, Albuquerque, New Mexico

Version of record first published: 09 Mar 2010.

To cite this article: John C. Duda , Patrick E. Hopkins , Justin L. Smoyer , Matthew L. Bauer , Timothy S. English , Christopher B. Saltonstall & Pamela M. Norris (2010): On the Assumption of Detailed Balance in Prediction of Diffusive Transmission Probability During Interfacial Transport, Nanoscale and Microscale Thermophysical Engineering, 14:1, 21-33

To link to this article: http://dx.doi.org/10.1080/15567260903530379

Nanoscale and Microscale Thermophysical Engineering, 14: 21–33, 2010

ISSN: 1556-7265 print / 1556-7273 online
DOI: 10.1080/15567260903530379

ON THE ASSUMPTION OF DETAILED BALANCE IN PREDICTION OF DIFFUSIVE TRANSMISSION PROBABILITY DURING INTERFACIAL TRANSPORT

John C. Duda[1], Patrick E. Hopkins[2], Justin L. Smoyer[1], Matthew L. Bauer[1], Timothy S. English[1], Christopher B. Saltonstall[1], and Pamela M. Norris[1]

[1]*Department of Mechanical and Aerospace Engineering, University of Virginia, Charlottesville, Virginia*

[2]*Engineering Sciences Center, Sandia National Laboratories, Albuquerque, New Mexico*

Models intended to predict interfacial transport often rely on the principle of detailed balance when formulating the interfacial carrier transmission probability. However, assumptions invoked significantly impact predictions. Here, we present six derivations of the transmission probability, each subject to a different set of preliminary assumptions regarding the type of scattering at the interface. Application of each case to phonon flux and thermal boundary conductance allows for a final quantitative comparison. Depending on the preliminary assumptions, predictions for thermal boundary conductance span over two orders of magnitude, demonstrating the need for transparency when assessing the accuracy of any predictive model.

KEY WORDS: detailed balance, diffuse scattering, thermal boundary conductance

INTRODUCTION

Modern nanostructured devices are engineered such that they meet a specific operational purpose. This is accomplished by manipulating the flow of pertinent carriers (i.e., electrons and/or phonons) through a particular material system and across the interfaces within that system. Consequently, interfacial transport is an ever-growing concern in a wide variety of disciplines, as continued reduction in the sizes of modern devices introduces more interfaces per unit length for a carrier to traverse. Regardless of the carrier type, the addition of interfaces will inevitably increase the total number of

The authors at U. Va. acknowledge the financial support of Office of Naval Research through a MURI grant (Grant No. N00014-07-1-0723) and the financial support of Air Force Office of Scientific Research (Grant No. FA9550-09-1-0245). J.C.D. is greatly appreciative for financial support from the National Science Foundation through the Graduate Research Fellowship Program. P.E.H. is grateful for funding from the LDRD program office through the Sandia National Laboratories Harry S. Truman Fellowship. Sandia is a multiprogram laboratory operated by Sandia Corporation, a Lockheed-Martin Company, for the United States Department of Energy's National Nuclear Security Administration under Contract DE-AC04-94AL85000.

Address correspondence to John C. Duda, Department of Mechanical and Aerospace Engineering, University of Virginia, 122 Engineer's Way, Charlottesville, VA 22904. E-mail: duda@virginia.edu

NOMENCLATURE

a	lattice constant
D	Debye density of states
f_0	equilibrium carrier distribution
$\hbar$	Planck's constant divided by 2π
h_{BD}	thermal boundary conductance
k	wavevector
q	interfacial flux
T	temperature

Greek Letters

ζ	transmission coefficient
θ	azimuthal angle relative to interface
ν	carrier group velocity
ϕ	elevation angle relative to interface
ω	phonon angular frequency

Subscripts

D	Debye model
j	polarization
x	in the x Cartesian direction, parallel to the interface
y	in the y Cartesian direction, parallel to the interface
z	in the z Cartesian direction, perpendicular to the interface
1	material or side 1
2	material of side 2

Superscripts

$1 \rightarrow 2$	from side 1 to side 2
$2 \rightarrow 1$	from side 2 to side 1

scattering events during transport processes. In some cases, an increase in scattering events is desired, whereas in others, it is not. For example, in thermoelectric devices, increased phonon scattering reduces thermal conductivity, leading to a greater overall figure of merit and better performance [1]. On the contrary, in transistors, increased electron scattering events lead to lower electron mobility, self-heating, and an increase in overall operating temperature, in turn reducing transistor speed and lifetime [2]. Regardless, it is important that accurate models exist when predicting interfacial transport, and that the assumptions of these models are well understood.

The development of any predictive model concerned with interfacial transport requires, before all else, a mathematical representation of flux across the interface. Thus, the flux, q, of any given quantity across an interface from side 1 to side 2, $b = b_j(k_x, k_y, k_z)$, whether that quantity is mass, charge, energy, or momentum, can be represented as

$$q_z^{1\rightarrow 2} = \frac{1}{(2\pi)^3}\sum_j \int_0^{\pi/2}\int_0^{2\pi}\int_{k_{x,1}}\int_{k_{y,1}}\int_{k_{z,1}>0} b_1 \zeta^{1\rightarrow 2}\nu_{j,1} f_0 \sin(\theta_1)\cos(\theta_1) dk_{z,1} dk_{y,1} dk_{x,1} d\theta_1 d\phi_1, \tag{1}$$

where z is the direction of transport, j is the polarization, θ_1 and ϕ_1 are the azimuthal and elevation angles of the flux on side 1 approaching side 2 relative to the direction of transport, ζ is the transmission coefficient, ν_1 is the carrier group velocity on side 1, f_0 is the equilibrium distribution of particles on side 1, and k is the wavevector. Here, k_z must be positive in order to only consider carriers approaching the interface. When the wavevectors $k_{x,1}$, $k_{y,1}$, and $k_{z,1}$ are collected as k_1 in subsequent analysis, this restriction on k_z is implied.

Equation (1) is derived by summing up the carrier flux moving toward the interface between sides 1 and 2 [3]. While this development is fairly straightforward, any

fundamental assumption invoked will have substantial implications on the formation of the transmission coefficient. To examine these implications we consider six different cases, each with a distinct set of assumptions regarding the type of scattering at the interface. The assumptions of each case are qualitatively discussed in the following section and the transmission coefficients are derived. In the next section, transmission coefficients are derived for phonon transport at interfaces within the context of each of these six cases. Then, phonon thermal boundary conductance is calculated, allowing for a quantitative comparison of the cases. We note that, under a very specific set of assumptions, the application of detailed balance to phonon transport produces the diffuse mismatch model (DMM) as presented by Swartz and Pohl [4]. In the literature, it has become common practice to use the DMM as a catch-all phrase for models addressing the diffusive transport of phonons across an interface. However, it will become clear by the end of this article that this may not be the best practice.

DETAILED BALANCE AND THE FORMATION OF THE TRANSMISSION COEFFICIENT

The principle of detailed balance requires that the interface of concern be in local equilibrium with sides 1 and 2. As a result, the flux from side 1 to side 2 across the interface must equal the flux from side 2 to side 1, or $q_z^{1\to2} = q_z^{2\to1}$. The expression for $q_z^{1\to2}$, as presented in Eq. (1), includes a transmission coefficient, ζ. By including ζ, we assume that a carrier moving from side 1 toward side 2 must scatter at the interface. The probability of the carrier traversing the interface between side 1 and side 2 after the scattering event is $\zeta^{1\to2}$, whereas the probability of the carrier scattering back into side 1 is $(1-\zeta^{1\to2})$.

In order to explicitly solve for $\zeta^{1\to2}$ we must, to an extent, assume diffuse scattering, such that $\zeta^{1\to2} = 1-\zeta^{2\to1}$. In the development of the following cases we switch between two assumptions, which we will call *complete diffuse scattering* and *partial diffuse scattering*. Complete diffuse scattering implies that incident carriers lose all memory of their initial direction and polarization after scattering at the interface. Thus, detailed balance is applied to the total flux incident at the interface. Partial diffuse scattering implies that incident carriers lose memory of their initial direction but not their polarization. Under this assumption, detailed balance is applied to the total flux *per polarization*. In both cases, carriers lose memory of their incident direction, allowing for integration over the azimuthal and elevation angles. This, in turn, reduces Eq. (1) to

$$q_z^{1\to2} = \frac{1}{8\pi^2}\sum_j \int\int\int_{k1} b_1\zeta^{1\to2}\nu_{j,1}f_0\ dk_1. \tag{2}$$

So far the only mention we have made to the 'type' of scattering at the interface has regarded the extent to which the diffuse assumption is applied. We can additionally vary the degree to which we assume elastic or inelastic scattering. During completely elastic scattering events, detailed balance must be applied *per wavevector*, such that a carrier on side 1 of the interface, $b_1(k_1)$, can only scatter with a carrier on side 2 of the interface, $b_2(k_2)$, if $b_1(k_1) = b_2(k_2)$. By integrating over k, this per wavevector

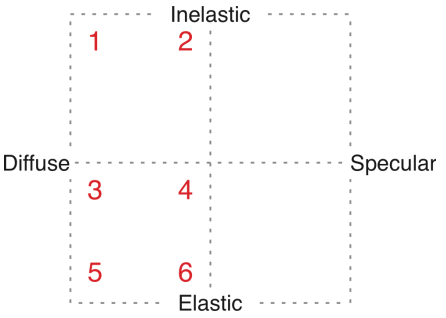

Figure 1. Schematic depicting where each of the six cases developed in the section detailed balance fall relative to the limits of the variable assumptions.

treatment is lost. However, the extent to which inelastic processes are considered depends, ultimately, on the range of carriers that participate during interfacial transport processes. For all six cases, we assume materials 1 and 2 are both isotropic. A schematic depicting where each case falls relative to the limits of the assumptions is shown in Figure 1.

Case 1, Balance of Total Flux

For case 1, we assume that interfacial scattering events are inelastic and completely diffuse. Application of detailed balance under these assumptions yields

$$\frac{1}{8\pi^2}\sum_j \int\int\int_{k_1} b_1 \zeta_{(\text{case1})}^{1\to 2} \nu_{j,1} f_0 dk_1 = \frac{1}{8\pi^2}\sum_j \int\int\int_{k_2} b_2 (1-\zeta_{(\text{case1})}^{1\to 2}) \nu_{j,2} f_0 dk_2. \quad (3)$$

Inelasticity is accounted for in Eq. (3) through two means: first, through the form of the integration limits, k_1 and k_2, and second, through the integration itself. The integration limits are determined only by the properties of materials 1 and 2, respectively; thus, all carriers on either side of the interface can participate, even when the population of allowable carrier states per wavevector is not the same in both materials. Second, by integrating over dk, interfacial transport is not calculated on a per wavevector basis, as an entirely elastic treatment would require. Additionally, this formulation is entirely diffuse due to the summarization over all polarizations, suggesting that a carrier of polarization j on side 1 can scatter with a carrier of polarization j' on side 2 at the interface between 1 and 2. Solving Eq. (3) for ζ yields a polarization independent transmission coefficient, given by

$$\zeta_{(\text{case1})}^{1\to 2} = \zeta^{1\to 2} = \frac{\sum_j \int\int\int_{k_2} b_2 \nu_{j,2} f_0 dk_2}{\sum_j \int\int\int_{k_2} b_2 \nu_{j,2} f_0 dk_2 + \sum_j \int\int\int_{k_1} b_1 \nu_{j,1} f_0 dk_1}. \quad (4)$$

Case 2, Balance of Flux per Polarization

For case 2 we assume that interfacial scattering events are inelastic and partially diffuse. This development implies that a carrier of polarization j on side 1 can only scatter with a carrier of the polarization j' on side 2 at the interface between 1 and 2 if $j = j'$. Thus, for case 2, application of detailed balance yields

$$\frac{1}{8\pi^2}\int\int\int_{k_1} b_1 \zeta^{1\to 2}_{(\text{case }2)} \nu_{j,1} f_0 dk_1 = \frac{1}{8\pi^2}\int\int\int_{k_2} b_2 \left(1 - \zeta^{1\to 2}_{(\text{case }2)}\right) \nu_{j,2} f_0 dk_2. \tag{5}$$

By applying detailed balance on a per polarization basis, the transmission coefficient must, in turn, be polarization specific. Solving Eq. (5) for ζ yields a transmission coefficient per polarization, given by

$$\zeta^{1\to 2}_{(\text{case }2)} = \zeta^{1\to 2}_{j} = \frac{\int\int\int_{k2} b_2 \nu_{j,2} f_0 dk_2}{\int\int\int_{k_2} b_2 \nu_{j,2} f_0 dk_2 + \int\int\int_{k_1} b_1 \nu_{j,1} f_0 dk_1}. \tag{6}$$

Despite the per polarization treatment, we have not imposed any carrier restrictions. Thus, case 2, like case 1, is inelastic.

Case 3, Balance of Total Flux Assuming Carrier Restrictions

Moving away from the inelastic assumption in cases 1 and 2, we now consider limiting which carriers can participate in interfacial transport. In most situations, the population of carriers per wavevector and allowable carrier states per wavevector is different in different materials. During inelastic interfacial transport this restriction is not of concern, because carriers of all wavevectors on either side of the interface can participate. For cases 3 and 4, we impose polarization-specific carrier restrictions by limiting the quantity of carriers that can participate. We integrate over $b_{j,\min}(k)$ when calculating the flux across the interface, where $b_{j,\min}(k)$ describes the carriers of the limiting material comprising the interface. Figure 2 illustrates fictitious dispersion relationships of the two materials, as well as how $b_{j,\min}(k)$ is determined.

For case 3 we return again to completely diffuse scattering and impose polarization-specific integration limits. The application of detailed balance yields

$$\frac{1}{8\pi^2}\sum_j \int\int\int_{k_1} b_{j,\min} \zeta^{1\to 2}_{(\text{case }3)} \nu_{j,1} f_0 dk_1 = \frac{1}{8\pi^2}\sum_j \int\int\int_{k_2} b_{j,\min} \left(1 - \zeta^{1\to 2}_{(\text{case }3)}\right) \nu_{j,2} f_0 dk_2. \tag{7}$$

Under these assumptions and this formulation of carrier restriction, case 3 can be described as quasielastic. An entirely elastic treatment would require the flux to be balanced per wavevector, whereas an inelastic treatment would have no carrier limits. As a result of the assumption of diffuse scattering and, hence, the summation over polarizations, the transmission coefficient is polarization independent, given by

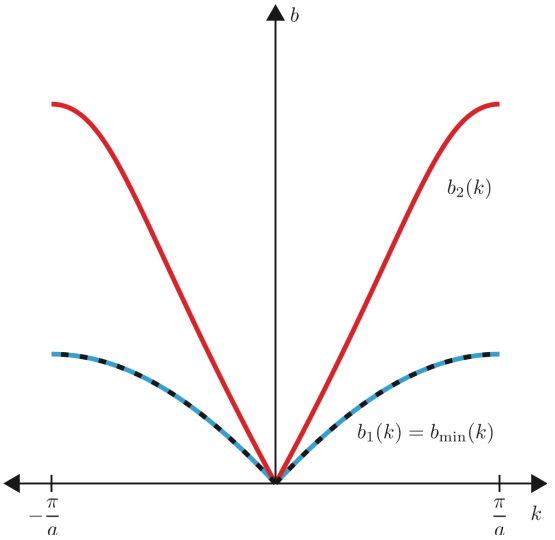

Figure 2. A representative dispersion diagram of two materials, where a given quantity, b, is a function of wavevector, k. When applying detailed balance in cases 1 and 2 we consider the entire quantity $b_1(k)$ in material 1 (red) and $b_2(k)$ in material 2 (blue). In cases 3 through 6, we only consider the restricted quantity $b_{\min}(k)$ that exists in both materials on either side of the interface. With regard to the above diagram, material 1 of the interface is the limiting material, thus $b_{\min}(k) = b_1(k)$. In cases 3 and 4, this restricted quantity is considered on a per polarization basis, whereas in cases 5 and 6, one single limiting quantity is considered for all polarizations.

$$\zeta^{1\to2}_{(\text{case3})} = \zeta^{1\to2} = \frac{\sum_j \int\int\int_{k_2} b_{j,\min}\nu_{j,2} f_0\, dk_2}{\sum_j \int\int\int_{k_2} b_{j,\min}\nu_{j,2} f_0 dk_2 + \sum_j \int\int\int_{k_1} b_{j,\min}\nu_{j,1} f_0 dk_1}. \quad (8)$$

Case 4, Balance of Flux per Polarization Assuming Carrier Restrictions

For case 4, we assume partially diffuse scattering and impose polarization specific integration limits. The application of detailed balance yields

$$\frac{1}{8\pi^2}\int\int\int_{k_1} b_{j,\min}\zeta^{1\to2}_{(\text{case4})}\nu_{j,1} f o dk_1 = \frac{1}{8\pi^2}\int\int\int_{k_2} b_{j,\min}(1-\zeta^{1\to2}_{(\text{case4})})\nu_{j,2} f_0 dk_2. \quad (9)$$

Subsequently, the polarization dependent transmission coefficient is given by

$$\zeta^{1\to2}_{(\text{case 4})} = \zeta^{1\to2}_j = \frac{\int\int\int_{k_2} b_{j,\min}\,\nu_{j,2} f_0 dk_2}{\int\int\int_{k_2} b_{j,\min}\,\nu_{j,2} f_0 dk_2 + \int\int\int_{k_1} b_{j,\min}\,\nu_{j,1} f_0 dk_1}. \quad (10)$$

Case 4, like case 3, can be considered quasi-elastic formulation for the reasons mentioned above.

Case 5, Balance of Flux per Wavevector Assuming Carrier Restrictions

For a completely diffuse and elastic treatment, where detailed balance is applied per wavevector, carrier restrictions must be the same for all polarizations, such that, $b_{j,\,\min}(k) = b_{\min}(k)$. For case 5, under these assumptions, the application of detailed balance yields

$$\frac{1}{8\pi^2}\sum_j b_{\min}\zeta^{1\to2}_{(\text{case }5)}\nu_{j,\,1}f_0\,dk_1 = \frac{1}{8\pi^2}\sum_j b_{\min}\left(1-\zeta^{1\to2}_{(\text{case }5)}\right)\nu_{j,\,2}f_0\,dk_2. \tag{11}$$

Again, the absence of integration over k suggests that flux is balanced on a per wavevector basis. The polarization-independent, wavevector-dependent transmission coefficient is given by

$$\zeta^{1\to2}_{(\text{case }5)} = \zeta^{1\to2}(k) = \frac{\sum_j b_{\min}\nu_{j,2}f_0\,dk_2}{\sum_j b_{\min}\nu_{j,2}f_0\,dk_2 + \sum_j b_{\min}\nu_{j,1}f_0\,dk_1}. \tag{12}$$

The transmission coefficient is a function of wavevector, k, such that a carrier on side 1 of the interface, $b_1(k_1)$, can only scatter with a carrier on side 2 of the interface, $b_2(k_2)$, if $b_1(k_1) = b_2(k_2)$.

Case 6, Balance of Flux per Polarization per Wavevector Assuming Carrier Restrictions

For case 6, we assume partially diffuse scattering and once again apply detailed balance on a per wavevector basis. Detailed balance, per polarization, per wavevector, yields

$$\frac{1}{8\pi^2}b_{\min}\zeta^{1\to2}_{(\text{case }6)}\,\nu_{j,1}f_0\,dk_1 = \frac{1}{8\pi^2}b_{\min}\left(1-\zeta^{1\to2}_{(\text{case }6)}\right)\nu_{j,2}f_0\,dk_2. \tag{13}$$

The polarization-dependent, wavevector-dependent transmission coefficient is given by

$$\zeta^{1\to2}_{(\text{case }6)} = \zeta^{1\to2}_j(k) = \frac{b_{\min}\,\nu_{j,2}f_0\,dk_2}{b_{\min}\,\nu_{j,2}f_0\,dk_2 + b_{\min}\,\nu_{j,1}f_0\,dk_1} \tag{14}$$

As in case 5, the transmission coefficient is a function of wavevector, k. However, the per polarization derivation requires that $b_{j,1}(k_1)$ can only scatter with a carrier on side 2 of the interface, $b_1(k_1) = b_2(k_2)$ if $j = j'$.

PHONON TRANSMISSIBILITY DURING INTERFACIAL TRANSPORT PROCESSES

For phonon interfacial transport, the quantity of concern, b, is the phonon energy, or $\hbar\omega$. In the following section we will take the transmission coefficients derived in the previons section and rewrite them in a form specific to phonons. From here onward, we assume that materials 1 and 2 are both Debye solids. Thus, $k = \omega/\nu$ and $dk = d\omega/\nu$, implying that phonon group velocity, ν is constant over the

entire Brillouin zone. We are interested only in phonon transport in the direction normal to the interface, z. As a result, the triple integral over wavevector is reduced to a single integral over k_2. From Eq. (2), the flux of phonon energy across the interface between two isotropic Debye solids perpendicular to the interface is given by

$$q_z^{1\to 2} = \frac{1}{8\pi^2}\sum_j \int_{k_{z,1}} \hbar\omega\big(k_{z,1}\big)k_{z,1}^2\,\zeta^{1\to 2}\nu_{j,1} f_0\, dk_{z,1} = \frac{1}{8\pi^2}\sum_j \nu_{j,1}^{-2}\int_{\omega_{j,1}} \hbar\omega^3\zeta^{1\to 2} f_0\, d\omega. \quad (15)$$

Through the application of detailed balance we determine phonon transmissibility across the interface from side 1 to side 2. Thus, in the context of the six cases presented above, the transmission coefficients are

$$\zeta_{(\text{case 1})} = \zeta^{1\to 2} = \frac{\sum_j \nu_{j,2}^{-2}\int_{\omega_{j,2}} \hbar\omega^3 f_0\, d\omega}{\sum_j \nu_{j,2}^{-2}\int_{\omega_{j,2}} \hbar\omega^3 f_0\, d\omega + \sum_j \nu_{j,1}^{-2}\int_{\omega_{j,1}} \hbar\omega^3 f_0\, d\omega}, \quad (16)$$

$$\zeta_{(\text{case 2})} = \zeta_j^{1\to 2} = \frac{\nu_{j,2}^{-2}\int_{\omega_{j,2}} \hbar\omega^3 f_0\, d\omega}{\nu_{j,2}^{-2}\int_{\omega_{j,2}} \hbar\omega^3 f_0\, d\omega + \nu_{j,1}^{-2}\int_{\omega_{j,1}} \hbar\omega^3 f_0\, d\omega}, \quad (17)$$

$$\zeta_{(\text{case 3})} = \zeta^{1\to 2} = \frac{\sum_j \nu_{j,2}^{-2}\int_{\omega_{j,1}} \hbar\omega^3 f_0\, d\omega}{\sum_j \nu_{j,2}^{-2}\int_{\omega_{j,1}} \hbar\omega^3 f_0\, d\omega + \sum_j \nu_{j,1}^{-2}\int_{\omega_{j,1}} \hbar\omega^3 f_0\, d\omega}, \quad (18)$$

$$\zeta_{(\text{case 4})} = \zeta_j^{1\to 2} = \frac{\nu_{j,2}^{-2}\int_{\omega_{j,1}} \hbar\omega^3 f_0\, d\omega}{\nu_{j,2}^{-2}\int_{\omega_{j,1}} \hbar\omega^3 f_0\, d\omega + \nu_{j,1}^{-2}\int_{\omega_{j,1}} \hbar\omega^3 f_0\, d\omega}, \quad (19)$$

$$\zeta_{(\text{case5})} = \zeta^{1\to 2} = \frac{\sum_j \nu_{j,2}^{-2}}{\sum_j \nu_{j,2}^{-2} + \sum_j \nu_{j,1}^{-2}}, \quad (20)$$

and

$$\zeta_{(\text{case6})} = \zeta_j^{1\to 2} = \frac{\nu_{j,2}^{-2}}{\nu_{j,2}^{-2} + \nu_{j,1}^{-2}}. \quad (21)$$

Though cases 5 and 6 are calculated on a per wavevector basis in Section 2, they are not presented on a per frequency basis here, because the frequency dependence is lost under the Debye assumption. It is also apparent that due to the absence of the distribution function, f_0, the case 5 and 6 transmission coefficients are not temperature dependent.

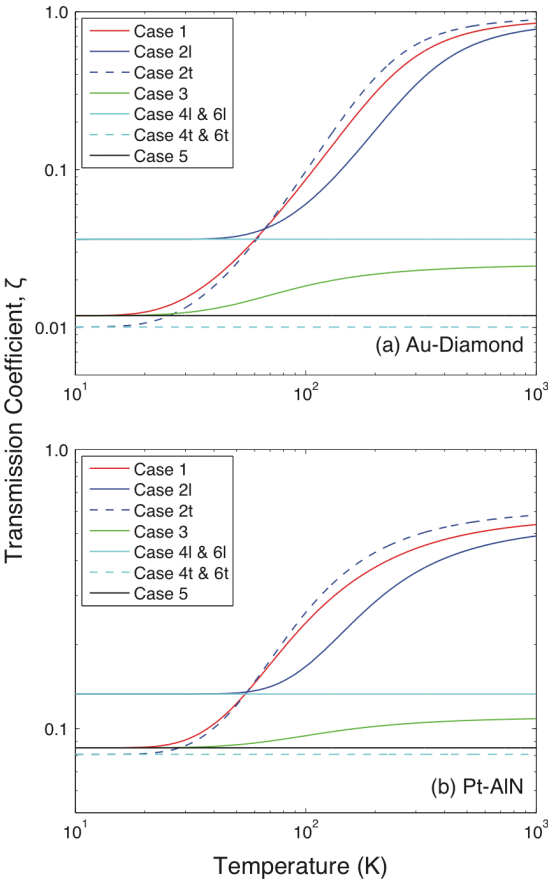

Figure 3. Illustration of the temperature dependence of ζ for (a) Au-diamond and (b) Pt-AelN interfaces. Note that there is one curve for each of the polarization-independent cases (1, 3, and 5). However, for the polarization-independent cases (2, 4, and 6) there are two curves per case, one longitudinal and one transverse. This assumes that the transverse modes are degenerate. Additionally, under the Debye assumption, cases 4 and 6 are degenerate.

Figure 3 illustrates the temperature dependence of ζ for both Au-diamond and Pt-AelN interfaces. There is one curve for each of the polarization independent cases (1, 3, and 5). However, for the polarization-independent cases (2, 4, and 6) there are two curves per case, one longitudinal and one transverse. This assumes that the transverse modes are degenerate. Additionally, under the Debye assumption, cases 4 and 6 are degenerate. For both material systems, the low-temperature degeneracy is apparent as the polarization-independent formulations (cases 1, 3, and 5) converge. This follows from the derivation above. The elastic–inelastic distinction ultimately changes the maximum phonon frequencies that participate in interfacial transport. At lower temperatures the distribution function dictates that few higher frequency phonons exist. Thus, a change in the upper limit of integration does not make a difference, as those higher frequency phonons are not present to participate.

Another interesting feature of Figure 3 is the influence of acoustic mismatch on the convergence and divergence of the different formulations of ζ; i.e., the difference between

maximum and minimum predictions of ζ at a given temperature. In this case, acoustic mismatch is defined as the ratio of the materials' Debye temperatures. The Deybe temperatures of Au, Pt, and diamond are 170, 230, and 1860 K, respectively [5], and that of AelN is 1020 K [6]. Thus, for the Au-diamond interface, the mismatch ratio is 0.091, and for the Pt-AIN interface, the ratio is 0.225. Not only do the different formulations of ζ converge more at low temperatures for heavily mismatched materials, but they diverge more at high temperatures. The increased divergence of mismatched materials is due to the significant difference in integration limits for the case of inelastic scattering. Mathematically, this is sound. Consider the fraction $b/(b+a)$. In the limit where $b \gg a, b/(b+a)$ goes to 1. In the limit where $b = a, b/(b+a)$ goes to 0.5. This, once again, stresses the role of the integration limits and, thus, how greatly the assumptions made during the application of detailed balance can change the accuracy of a model.

APPLICATION TO THERMAL BOUNDARY CONDUCTANCE

Assuming an interface can be described by some finite thermal conductance, a thermal flux across the interface will establish a temperature drop. Thermal boundary conductance is the rate at which energy traverses an interface per unit area per degree temperature drop and is often expressed in units of $\mathrm{W\,m^{-2}K^{-1}}$. Phonon thermal boundary conductance, h_{BD}, can be calculated by recognizing that

$$q_z^{1\to 2} = h_{\mathrm{BD}}^{1\to 2}\Delta T \Rightarrow h_{\mathrm{BD}}^{1\to 2} = \frac{\partial q_z^{1\to 2}}{\partial T}. \tag{22}$$

Taking the partial derivative of Eq. (15) with respect to temperature yields

$$h_{\mathrm{BD}}^{1\to 2} = \frac{1}{4}\sum_{j}^{3}\int_0^{\omega_{D,j}} \zeta^{1\to 2}\hbar\omega\nu_{1,j}D(\omega,\nu_{1,j})\frac{\partial}{\partial T}f_0 d\omega, \tag{23}$$

which is the general form of the DMM originally presented by Swartz and Pohl [4]. It is important to remember when calculating h_{BD} via Eq. (23) that the same assumptions made during the formulation of the transmission coefficient must continue to be upheld. That is, the maximum frequency over which we integrate $\omega_{\mathrm{D},j}$ will be dependent on the formulation of ζ.

Many of the formulations of ζ presented in the previous section have appeared in the literature within the context of predicting h_{BD} via the DMM. Swartz and Pohl's derivation of the DMM followed the assumptions outlined by case 5, where scattering is both completely diffuse and completely elastic [4]. However, since that development, the assumptions made during the application of detailed balance have been tailored by others for different reasons. For example, both Dames and Chen [7] and Hopkins and Norris [8] developed the DMM under the assumptions of case 1, where scattering is completely diffuse and completely inelastic. This development was performed in the context of acoustically mismatched interfaces. Experimental evidence suggests that in elastic scattering plays a significant role for these interfaces at elevated temperatures [9]. A completely diffuse, quasi-elastic treatment analogous to case 3 was implemented by Duda *et al.* for predicting h_{BD} at metal-graphite interfaces [10]. This approach was taken to ensure all incident flux was considered, limiting any under prediction of

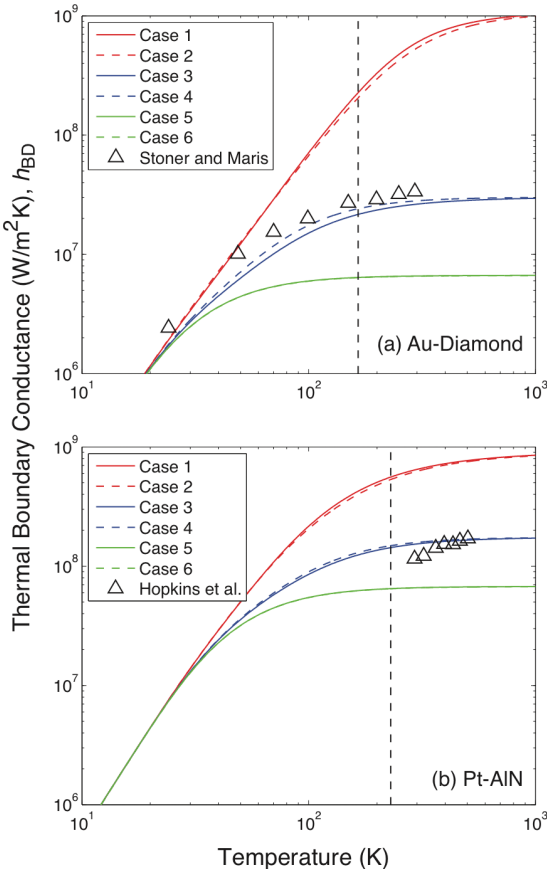

Figure 4. The temperature dependence of h_{BD} for (a) Au-diamond and (b) Pt-AelN interfaces. Aueldiamond [12] and Pt-AIN [9] have been taken from literature for comparison. Immediately noticeable in both material systems is that the polarization-dependent or independent distinction does not make a significant difference in the predicted value of h_{BD}. The dashed line represents the Debye temperature of the material comprising side 1. Cases 5 and 6, as expected, level off past the Debye temperature of material 1.

experimental data. Hopkins [11] used a partially diffuse, quasi-elastic treatment analogous to case 4 to ensure the conservation in phonon population when modeling the role of multiple-phonon processes during interfacial transport processes.

Figure 4 shows the temperature dependence of h_{BD} for Au-diamond and Pt-AIN interfaces as predicted by Eq. (23) for each case above and compares these predictions to experimental data. One thing that is immediately noticeable in both material systems is that the polarization-dependent or independent distinction does not make a significant difference in the predicted value of h_{BD}. That is, for both the Au-diamond and Pt-AIN material systems, there is some level of degeneracy between cases 1 and 2, cases 3 and 4, and cases 5 and 6. For both of these interfaces, these plots demonstrate that the interfacial transport occurs in a regime somewhere between the lower elastic and upper inelastic limits. However, both the upper and lower limits seem to falter when considering a realistic description of phonon scattering at the interface.

The upper limit presented by cases 1 and 2 considers total inelastic scattering in such a way to suggest that if two carriers can scatter inelastically, they will. That is, there is no

probability associated with the likelihood that multiple carriers, in this case phonons, will overlap in space and time, thus allowing for an inelastic process to occur. It is reasonable to assume that the chances for higher-order phonon processes decreases as the number of phonons required by the process increases. Thus, it is reasonable to expect cases 1 and 2 to over predict measured h_{BD}. On the other hand, the lower limit presented by cases 5 and 6 considers only elastic scattering processes in such a way that the upper integration limit in Eqs. (15) and (23) is the lowest of the cutoff frequencies for each polarization. For example, if the cutoff frequency for one polarization is lower than another polarization, as is often the case with the transverse and longitudinal polarizations, only phonons up to the lowest maximum frequency are considered. Essentially, this ignores a discrete, and sometimes significant, amount of phonon thermal flux approaching the interface. Limitations are put on the flux approaching the interface, even if the range of ignored phonon frequencies exists in the material on the other side of the interface. As a result, it is reasonable that cases 5 and 6 will under predict measured h_{BD}.

We believe that cases 3 and 4 are the most reasonable, because they do not ignore any incident flux, nor do they assume that less-probable three-phonon-and-higher inelastic scattering processes dominate interfacial transport. However, assessing which of these two cases is the single most appropriate is more difficult. Despite the different formulations, we note that, for the material systems considered, cases 3 and 4 are nearly degenerate. As a result, it is impossible to tell with any certainty whether the loss of memory with regard to polarization is an valid assumption. Further experimental data, looking specifically at material systems where the cutoff frequencies for each polarization differ significantly, could provide more insight.

CONCLUSION

Through the application of detailed balance, transmission coefficients have been derived under different sets of assumptions, focusing primarily on the elastic-inelastic and specular-diffuse distinctions. The six cases discussed have been presented generally in k-space, thus reaffirming that such a development can be applied to any type of particle carrying any quantity, whether that quantity is mass, charge, energy, or momentum. These cases are subsequently applied to interfacial phonon transport such that differences between the cases can be quantified. Lastly, the diffuse mismatch model is used as an example to demonstrate the significant impact of the assumptions of detailed balance when predicting diffusive transmission probability during interfacial transport. Though traditionally case 5 has described the assumptions most widely used when formulating the DMM, it has been shown that these may not best describe interfacial phonon transport for all situations. Thus, it is important to ensure that assumptions made during the application of detailed balance accurately reflect the scattering conditions at the interface of interest.

REFERENCES

1. L.W. da Silva and M. Kaviany, Micro-Thermoelectric cooler: Interfacial Effects on Thermal and Electrical Transport, *International Journal of Heat and Mass Transfer*, vol. 47, p. 241, 2004.
2. S.M. Sze and K.K. Ng, *Physics of Semiconductor Devices*, Wiley, Hoboken, NJ, 2007.
3. G. Chen, *Nanoscale Energy Transport and Conversion: A Parallel Treatment of Electrons,. Molecules, Phonons, and Photons*, Oxford University Press, New York, 2005.

4. E.T. Swartz and R.O. Pohl, Thermal Boundary Resistance, *Reviews of Modern Physics*, vol. 61, p. 605, 1989.
5. N.W. Ashcroft and N.D. Mermin, *Solid State Physics*, Thomson Learning, 1976.
6. J.C. Nipko and C.-K. Loong, Phonon Excitations and Related Thermal Properties of Aluminum Nitride, *Physical Review* B, vol. 57, p. 10550, 1998.
7. C. Dames and G. Chen, Theoretical Phonon Thermal Conductivity of Si/Ge Superlattice Nanowires, *Journal of Applied Physics*, vol. 95, p. 682, 2004.
8. P.E. Hopkins and P.M. Norris, Relative Contributions of Inelastic and Elastic Diffuse Phonon Scattering to Thermal Boundary Conductance across Solid Interfaces, *Journal of Heat Transfer*, vol. 131, p. 022402, 2009.
9. P.E. Hopkins, P.M. Norris, and R.J. Stevens, Influence of Inelastic Scattering at Metal-Dielectric Interfaces, *Journal of Heat Transfer*, vol. 130, p. 022401, 2008.
10. J.C. Duda, J.L. Smoyer, P.M. Norris, P.E. Hopkins, Extension of the Diffuse Mismatch Model for Thermal Boundary Conductance between Isotropic and Anisotropic Materials, *Applied Physics Letters*, vol. 95, p. 031912, 2009.
11. P.E. Hopkins, Multiple Phonon Processes Contributing to Inelastic Scattering during Thermal Boundary Conductance at Solid Interfaces, *Journal of Applied Physics*, vol. 106, p. 013528, 2009.
12. R.J. Stoner and H.J. Maris, Kapitza Conductance and Heat Flow between Solids at Temperature from 50 to 300 k, *Physical Review B*, vol. 48, p. 16373, 1993.